JOURNAL OF GEOPHYSICAL RESEARCH, VOL. 111, C04009, doi:10.1029/2005JC003232, 2006

On the accuracy of HF radar measurement in the Tsushima Strait

Y. Yoshikawa,[1] A. Masuda,[1] K. Marubayashi,[1] M. Ishibashi,[1] and A. Okuno[2]

Received 18 August 2005; revised 11 December 2005; accepted 19 January 2006; published 22 April 2006.

[1] The accuracy of HF radar measurement in the Tsushima Strait is investigated. A comparison between radial velocities measured by HF radar and acoustic Doppler current profiler (ADCP), which provides an upper bound of HF radar measurement error, shows that the root-mean-square (RMS) velocity difference obtained from the principal component analysis is $6.62 \sim 11.3$ cm s^{-1}. A comparison of velocities measured by two facing HF radars, which provides a lower bound of HF radar measurement error, shows that the variance error of hourly radial velocity is $5.75 \sim 13.3$ cm s^{-1}. The bias error of HF radar measurement is also found to be reasonably small through a comparison of tidal ellipses estimated from 1 year of HF radar data with those from 5 years of ADCP data. These results suggest that the variance error of HF radar measurement is the dominant source of the velocity difference found between ADCP and HF radar.

Citation: Yoshikawa, Y., A. Masuda, K. Marubayashi, M. Ishibashi, and A. Okuno (2006), On the accuracy of HF radar measurement in the Tsushima Strait, *J. Geophys. Res.*, *111*, C04009, doi:10.1029/2005JC003232.

1. Introduction

[2] The Tsushima Strait is located between Japan and Korea and connects the East China Sea and the Japan Sea (Figure 1). Through this strait, warm and saline subtropical waters of the East China Sea and the Pacific Ocean are transported into the southern Japan Sea. The Tsushima Strait is thus a suitable place to monitor a major source of hydrographic variabilities in the southern Japan Sea, and hence many studies have been conducted to better understand current and hydrographic structures in the Tsushima Strait [*Takikawa et al.*, 2003, and references therein].

[3] The mean current from the East China Sea into the Japan Sea is called the Tsushima Warm Current. Long-term measurement with an acoustic Doppler current profiler (ADCP) mounted on a ferryboat across the Tsushima Strait reveals large seasonal variation of this current [*Takikawa et al.*, 2003]. Tidal currents are as strong as the Tsushima Warm Current in this shallow (~200 m) strait [*Odamaki*, 1989; *Takikawa et al.*, 2003]. Strong northwesterly monsoon wind in the winter drives a surface flow to the south or southeast. The Tsushima and Iki islands further complicate this current system. Thus current variabilities are expected to be very high in this strait. However, only a small fraction of these variabilities have been investigated in a quantitative manner. One reason for this lack is the large number of very active fisheries in this strait, which make long-term current meter mooring impracticable. Another reason is the highly complex nature of the current variabilities, which require large numbers of data to isolate each component of the variabilities.

[4] A high frequency ocean radar (hereafter HF radar) is a still developing and recently accepted instrument that probes surface currents remotely from the coast [e.g., *Paduan and Graber*, 1997]. It can measure surface currents at short intervals (every about one hour), for a long period (longer than several months), and over a large area ($\sim$1000 km^2). This capability enables quantitative understanding of the complicated current systems in the Tsushima Strait. To this aim, we deployed seven HF radars in the Tsushima Strait in February 2002. Many interesting variabilities, such as an anticlockwise eddy in the eastern channel of the strait (Figure 2), are found by this HF radar measurement. Details of these variabilities and their associated dynamics will be described in a future paper.

[5] Several studies [*Holbrook and Frisch*, 1981; *Matthews et al.*, 1988; *Chapman et al.*, 1997; *Graber et al.*, 1997; *Nadai et al.*, 1997] have investigated the accuracy of HF radar measurement. These studies examined the velocity difference between HF radar and current meter (such as ADCP) measurements and found that the root-mean-square of this difference is $\sim$15 cm s^{-1}. It should be noted that this difference can be written as

$$v^{\mathrm{HFOR}} - v^{CM} = \left(v^{\mathrm{HFOR}} - \overline{v}^{\mathrm{HFOR}}\right) - \left(v^{CM} - \overline{v}^{CM}\right) + \left(\overline{v}^{\mathrm{HFOR}} - \overline{v}^{CM}\right),$$

where v^{HFOR}, v^{CM} are velocities that are actually measured by HF radar and a current meter respectively, and $\overline{v}$ denotes velocity that should be measured without measurement error. Thus the velocity difference is composed of three sources: HF radar measurement error ($v^{\mathrm{HFOR}} - \overline{v}^{\mathrm{HFOR}}$), current meter measurement error ($v^{CM} - \overline{v}^{CM}$), and the difference between what HF radar should measure and what

[1]Research Institute for Applied Mechanics, Kyushu University, Kasuga, Fukuoka, Japan.

[2]National Research Institute of Fisheries Science, Fisheries Research Agency, Yokohama, Kanagawa, Japan.

Copyright 2006 by the American Geophysical Union.
0148-0227/06/2005JC003232$09.00

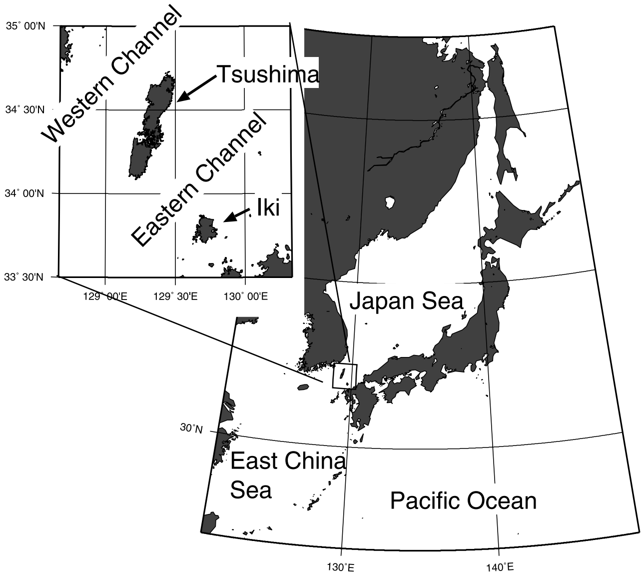

Figure 1. Location and geographical configuration of the Tsushima Strait.

the current meter should measure ($\overline{v}^{\mathrm{HFOR}} - \overline{v}^{CM}$). The third source comes from the fact that HF radar should measure average velocity over a large area ($\sim$ a few km^2) near the surface ($\sim$1 m), while the current meter should measure velocity at a single point at a greater depth ($\geq$ a few meters). For the sake of simplicity, we refer to the third source as target difference. The problems here are that the target difference is not easy to estimate with good accuracy, and that it might be large. As a result, HF radar measurement error, which is obtained from the (measured) velocity difference minus the (estimated) target difference, is rarely estimated with good accuracy.

[6] The purpose of this study is to quantitatively examine the accuracy of HF radar measurement in the Tsushima Strait. To this aim, we compare not only radial velocities measured by HF radar and ADCP, as in the previous studies, but also radial velocities measured by two facing HF radars [e.g., *Lipa*, 2003; *Paduan et al.*, 2006]. In the following, the HF radar data and ADCP data used in this study are described in section 2. Velocities measured by HF radar are compared with those measured by ADCP in section 3. A comparison between velocities measured by the two facing HF radars is described in section 4. The variance and bias errors of the HF radar measurement are discussed in section 5. Finally, a summary is given in section 6.

2. Data Source

2.1. HF Radar

[7] In February 2002, five HF radars were installed in the Tsushima Strait, and their number later increased from five (after February 2002) to seven (after July 2003). The location of the radar sites, their looking lines, and their range coverage are shown in Figure 3. Two types of HF radar, CODAR (C1$\sim$C5) and NJRC (N1$\sim$N2), were installed.

[8] CODAR is a unique system that employs two crossed loop antennas around a whip (vertical monopole) as a receiving antenna and two whips as a transmitting antenna [*Barrick et al.*, 1997]. This system is very compact and only requires a small area for its deployment. The direction finding method is adopted in this system [*Lipa and Barrick*, 1983; *Barrick and Lipa*, 1997]. In this method, distortion of the antenna pattern by the surroundings results in bias error of the bearing angle from which the received signal comes. In this study, the measured antenna pattern was used (except in section 5) to minimize such bias error. CODAR transmits

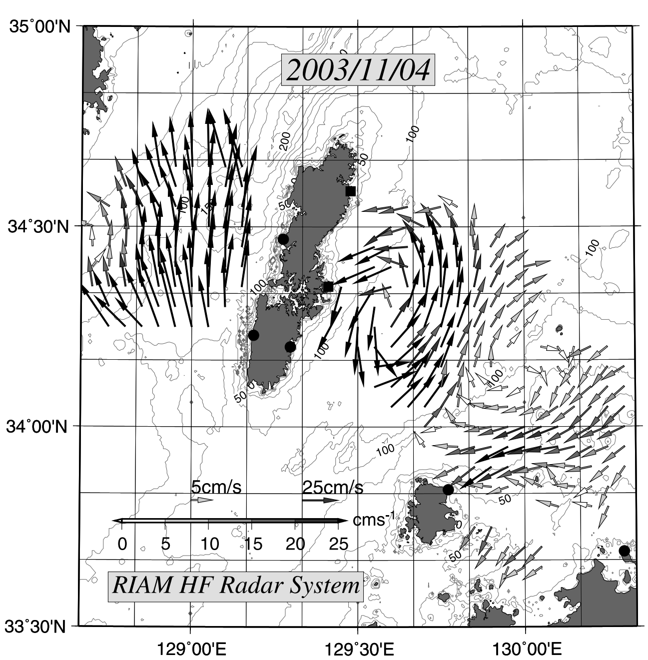

Figure 2. Example of anticlockwise eddy observed in the eastern channel of the Tsushima Strait.

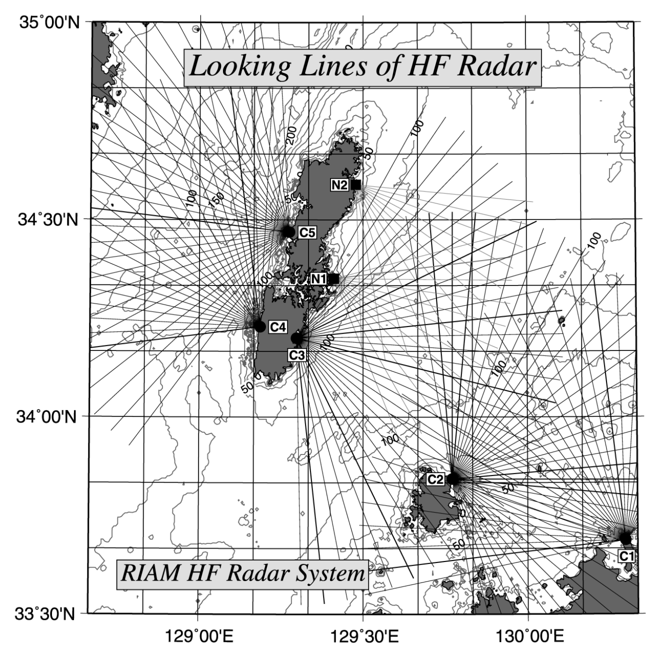

Figure 3. Location of HF radar sites (CODAR, C1$\sim$C5; NJRC, N1 and N2). Looking lines and range coverage of each radar are drawn by lines.

Table 1. Specifications of HF Radars in the Tsushima Strait

	Radar Type	
	CODAR	NJRC
Tx antenna	two mono pole antennas	one Yagi antenna
Rx antenna	crossed loop/mono pole antenna	eight Yagi antennas
Center frequency, MHz	13.9	24.5
Sweep bandwidth, kHz	49	100
Sweep rate, Hz	2.0	2.0
Range coverage, km	75	50
Bearing coverage, deg	360	90
Range resolution, km	3.0	1.5
Bearing resolution, deg	5	7.5
Measurement depth, m	∼1.72	∼0.98

signals continuously, and thus a GPS synchronization system was employed to prevent interference between CODARs. CODAR samples 512 sweeps for 256 s to obtain cross spectra data, which are averaged every 10 min to estimate the radial velocity and then combined every hour to get the hourly radial velocity.

[9] NJRC is a type of linear array antenna system using the digital beam forming technique. It consists of one transmitting Yagi antenna and eight receiving Yagi antennas. Until May 2003, NJRC sampled 2400 sweeps for 20 min to obtain cross spectra data, and two NJRC radars operated alternatively (N1:35∼55 min, N2 05∼25 min) to prevent interference between them. In May 2003, a GPS synchronization system was also installed into the NJRC system. Thereafter, NJRC samples 3600 sweeps for 30 min to obtain cross spectra data, and two NJRC radars operate almost simultaneously (N1: 14∼44 min, N2 16∼46 min), although the measurement interval is still one hour. The radial velocity is estimated every hour. Further details of the specifications of each radar type are listed in Table 1.

2.2. ADCP

[10] Several types of current data measured by the ADCPs were used in this study (Table 2). One type is that measured by the ADCP (RD Inc., 150 kHz) towed by the training vessel *Kakuyo-Maru* of Nagasaki University, which measures currents deeper than approximately 13 m from the surface with 2 m bin size. The second type is that measured by the ADCP (RD Inc., 600 kHz) mounted on the research boat *Danryu*, which measures currents deeper than 2 m with 1 m bin size. Both ADCPs measure in the bottom track mode, and the error of ADCP measurement is generally thought to be less than a few centimeters per second. The locations of these ADCP measurements are shown in Figure 4a. Although these ADCPs give relatively accurate current velocities, the amount of data was not large (the number of velocity data measured by T/V *Kakuyo-Maru* and R/B *Danryu* were 67 and 49, respectively), and thus good statistical accuracy could not be expected. To increase the ensemble number of samples, the current velocities at 13 m depth measured by R/B *Danryu* were used together with those measured by T/V *Kakuyo-Maru* for the comparison with HF radar velocities. Further, for the comparison over a wider area with much larger statistical accuracy, we also used ADCP data of the 7th Regional Coast Guard Headquarters (RCGH) and the Fukuoka Fisheries and Marine Technology Research Center (FFMTRC). The ADCP (Furuno Inc., 150 kHz) is mounted on patrol ships or research ships and measures only three levels (typically greater than 5 m depth). In this study, the shallowest data between 5∼9 m obtained in the bottom track mode was used. T/V *Kakuyo-Maru* is also equipped with this ADCP (Furuno

Table 2. Summary of ADCP Measurements

Data Source	ADCP (Frequency, kHz)	Depth, m	Corresponding Radar
R/B *Danryu*	RD (600 kHz)	>2	C1, C2
T/V *Kakuyo-Maru*	RD (150 kHz)	>13	C1, C2, N1, N2
	Furuno (150 kHz)	>7	C1 ∼ C5, N1, N2
7th RCGH	Furuno (150 kHz)	>5	C1 ∼ C5, N1, N2
FFMTRC	Furuno (150 kHz)	>5	C1 ∼ C3, N1, N2

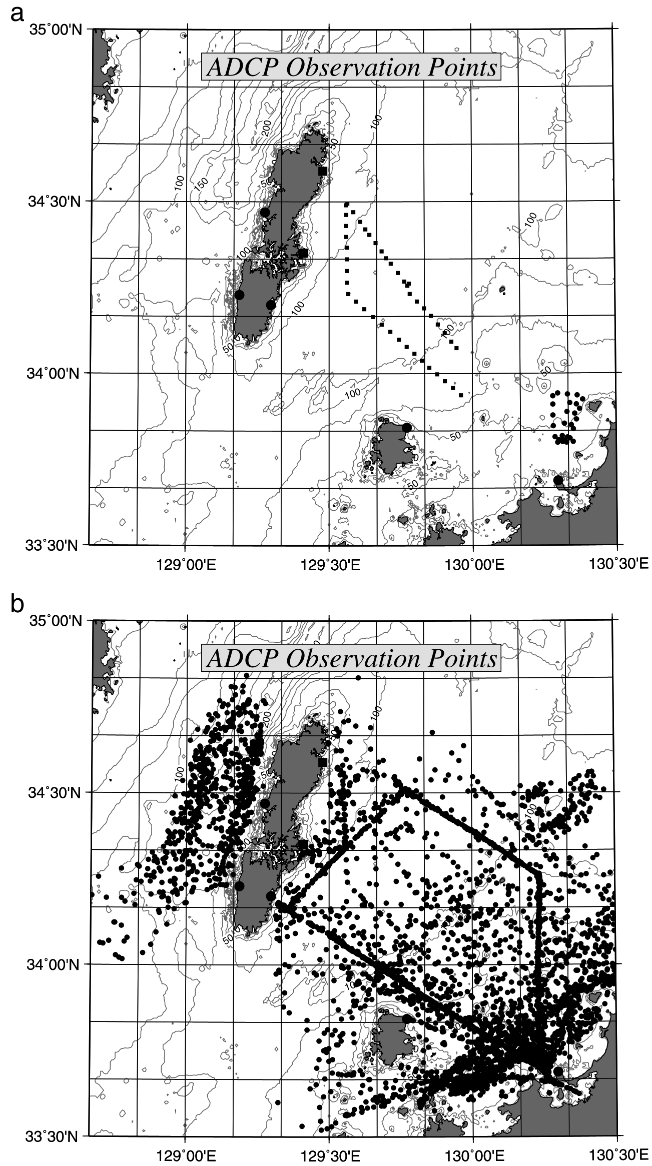

Figure 4. Locations of ADCP measurements. (a) ADCP (RD Inc., 150 kHz) towed by T/V *Kakuyo-Maru* (square) and ADCP (RD Inc., 600 kHz) mounted on R/B *Danryu* (circle). (b) ADCP (Furuno Inc., 150 kHz) mounted on T/V *Kakuyo-Maru*, patrol ships of 7th RCGH, and research ships of FFMTRC.

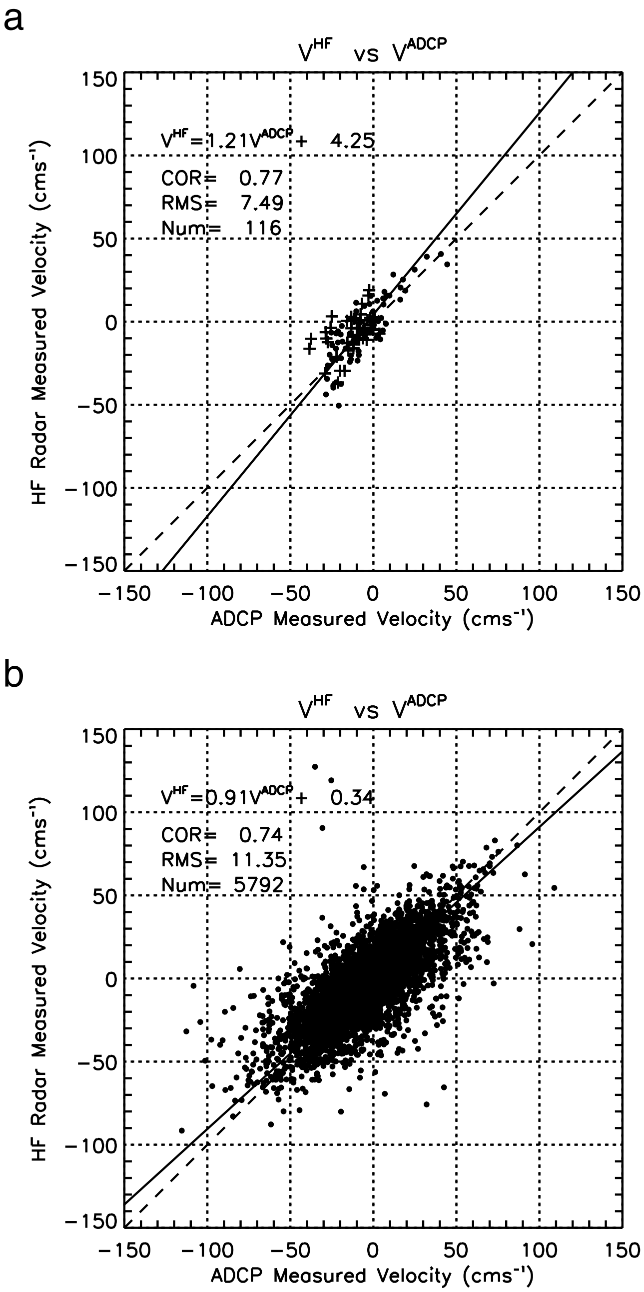

Figure 5. Scatterplots of ADCP measured velocity (horizontal axis) and HF radar measured velocity (vertical axis). (a) ADCP (RD Inc., 150 kHz) towed by T/V *Kakuyo-Maru* (circle) and ADCP (RD Inc., 600 kHz) mounted on R/B *Danryu* (plus). Data at 13 m depth were used. (b) ADCP (Furuno Inc., 150 kHz) mounted on T/V *Kakuyo-Maru*, patrol ships of 7th RCGH, and research ships of FFMTRC. Shallowest data at 5∼9 m depth were used. Solid line is the regression line obtained with PCA.

Inc., 150 kHz), and thus its data was also used in this study. Unfortunately, the recording unit of the velocity magnitude of the Furuno ADCP is only 0.1 knot ($\simeq$5.1 cm s^{-1}), and therefore measurement accuracy can be expected to be worse than the RD ADCP. However, the measurements were done many times over a wide area of the HF radar measurement region (Figure 4b) so that these ADCP data can be useful in validating the HF radar measurements.

[11] All ADCP data were averaged every 20 min, corresponding to a 3∼6 km spatial average for typical ship speed. The velocity vector was projected to the radial component of each radar site to be compared with the radial velocity measured by each HF radar.

3. Comparison With ADCP

[12] Figure 5 shows the scatterplots of the ADCP-measured velocity (v^{ADCP}, horizontal axis) and HF-radar-measured velocity (v^{HFOR}, vertical axis). The solid line is the regression line obtained from the principal component analysis (PCA) which minimizes the sum of the square distance from the point (x, y) to the regression line ($y = Ax + B$) on the $x - y$ plane. The regression coefficients (A and B), correlation (COR), root-mean-square distance (RMS), and number of samples (NUM) are listed in Table 3. Note that PCA is used for the regression line estimates throughout this study. This is partly because two variables (velocities measured by HF radar and ADCP in this section) have errors, and partly because PCA provides the symmetric regression line with respect to the two variables in scatterplots. This feature is particularly important when two HF radar velocities are compared in section 4. Note the difference between the definition of RMS in this study and that in the previous studies, in which the simple root-mean-square of "difference" ($v^{HFOR} - v^{ADCP}$, hereafter simply referred to as SDV) is used. If the slope of the regression line is close to unity (as in the present study), then RMS is about $\sqrt{2}$ times smaller than SDV. This corresponds to the fact that the variance of difference between x and y includes the variance errors of both x and y ($\sigma^2 = \sigma_x^2 + \sigma_y^2$) if these errors are independent of each other. When $\sigma_x \simeq \sigma_y$, then $\sigma_x \simeq \sigma/\sqrt{2}$, which corresponds to the variance obtained from PCA. Thus RMS obtained from PCA in this study corresponds to the variance error of a single measurement system. Though all discussions are based on RMS in the present study, SDVs are also listed in Tables 3 and 4 for easy comparison with previous studies.

[13] Partly because of its smaller statistical error (i.e., larger number of samples) and partly because of its shallower measurement depth (5∼9 m), the regression coefficients of the Furuno ADCP (A = 0.91, B = 0.34 cm s^{-1}) are better than those of the RD ADCP (A = 1.20, B = 3.36 cm s^{-1}). The RMS of the RD ADCP (6.62 cm s^{-1}) is smaller than that of the Furuno ADCP (11.3 cm s^{-1}), and this is due mainly to the better measurement accuracy of the former. Statistics obtained with the Furuno ADCP do not change significantly

Table 3. Comparison Statistics Between ADCP-Measured Velocity v^{ADCP} and HF-Radar-Measured Velocity v^{HFOR} [a]

ADCP	Depth, m	Radar	A	B, cm s^{-1}	COR	RMS, cm s^{-1}	SDV, cm s^{-1}	NUM
RD	13	C1, C2, N1, N2	1.20	3.36	0.82	6.62	9.89	111
Furuno	5∼9	ALL	0.91	0.34	0.74	11.3	16.2	5792
	5∼9	C1∼C5	0.90	0.51	0.75	11.4	16.3	5140
	5∼9	N1, N2	0.98	−0.92	0.70	10.6	15.0	652

[a] A, B, slope and intercept of regression line obtained with PCA; COR, correlation coefficient; RMS, root-mean-square distance from regression line; SDV, root-mean-square of velocity difference; NUM, number of samples.

Table 4. Same as Table 3 but for Comparison Between Radial Velocities Measured by Two Facing Radars[a]

Radar Pair	Period	*A*	*B*, cm s^{-1}	COR	RMS, cm s^{-1}	SDV, cm s^{-1}	NUM
C1 − C2	Feb 2002 to Apr 2005	0.91	0.28	0.88	5.75	8.26	27,095
		(1.00)	(−3.45)	(0.86)	(7.13)	(10.7)	(24,163)
C1 − C3	Jul 2003 to Apr 2005	1.00	−0.90	0.63	13.7	19.4	11,949
		(1.09)	(1.80)	(0.63)	(12.5)	(17.9)	(12,576)

[a]Values in parentheses represent statistics between velocities estimated with an ideal antenna pattern.

even though CODAR and NJRC are compared separately (Table 3), suggesting that both radar have similar measurement accuracy. The SDVs obtained in this study are comparable to those of previous studies, indicating that the measurement accuracy of HF radars in the Tsushima Strait is also similar to that of previous studies.

4. Comparison With Facing HF Radar

[14] The RMS of the order of 10 cm s^{-1} is not so small in the Tsushima Strait, where typical current speed is about 50 cm s^{-1}, and therefore further investigation of the source of the difference is done in this section.

[15] As described in section 1, there are three sources of errors or difference in RMS: HF radar measurement error, ADCP measurement error, and the target difference. Thus RMS obtained from the comparison with ADCP is an upper bound of HF radar measurement error. In some cases, the target difference is so large that the HF radar measurement error may be much smaller than the RMS obtained from comparison with ADCP. How large is the actual target difference and how small is HF radar measurement error?

[16] In order to give an answer to this question, we attempted to quantify the HF radar measurement error rather than estimate the target difference. For this purpose, the velocities measured by the two facing HF radars along their baseline were compared. In this comparison, the target difference is negligible if the comparison is made at the middle of baseline and if the electromagnetic wave frequencies of the two radars are the same. Because bias error is partly cancelled, variance error (RMS) and a part of the bias error of HF radar measurement are obtained from this comparison. A comparison of the radial velocities of two facing radars has also been made independently by *Lipa* [2003] and *Paduan et al.* [2006].

[17] In the Tsushima Strait, there are two pairs (C1–C2 and C1–C3) of radars appropriate for this comparison. Figure 6 shows scatterplots of hourly radial velocities at the middle point of C1–C2 (obtained from 1 February 2002 to 30 April 2005) and C1–C3 (obtained from 1 July 2003 to 30 April 2005). Regression coefficients (A,B), correlation (COR), RMS, SDV, and number of samples (NUM) are listed in Table 4. The regression coefficients from the C1–C2 pair (A = 0.91, B = 0.28 cm s^{-1}) show that the amplitude of velocity variation is about 10% larger for C1 than for C2. On the other hand, the regression coefficients for the C1–C3 pair (A = 1.00, B = −0.90 cm s^{-1}) are quite reasonable. The bias error between C1 and C2 is related to antenna pattern distortion that is not perfectly corrected in spite of the use of the measured antenna pattern (described in detail in section 5). The correlation (0.88) and RMS (5.75 cm s^{-1}) between C1 and C2 seem reasonable judging from the velocity resolution of the HF radar measurement (a few centimeters per second), while the correlation (0.63) and RMS (13.7 cm s^{-1}) between C1 and C3 are worse than those for the C1–C2 pair. The larger scatter between C1 and C3 might be related to the longer distance between them because the signal-to-noise ratio becomes worse as the distance from

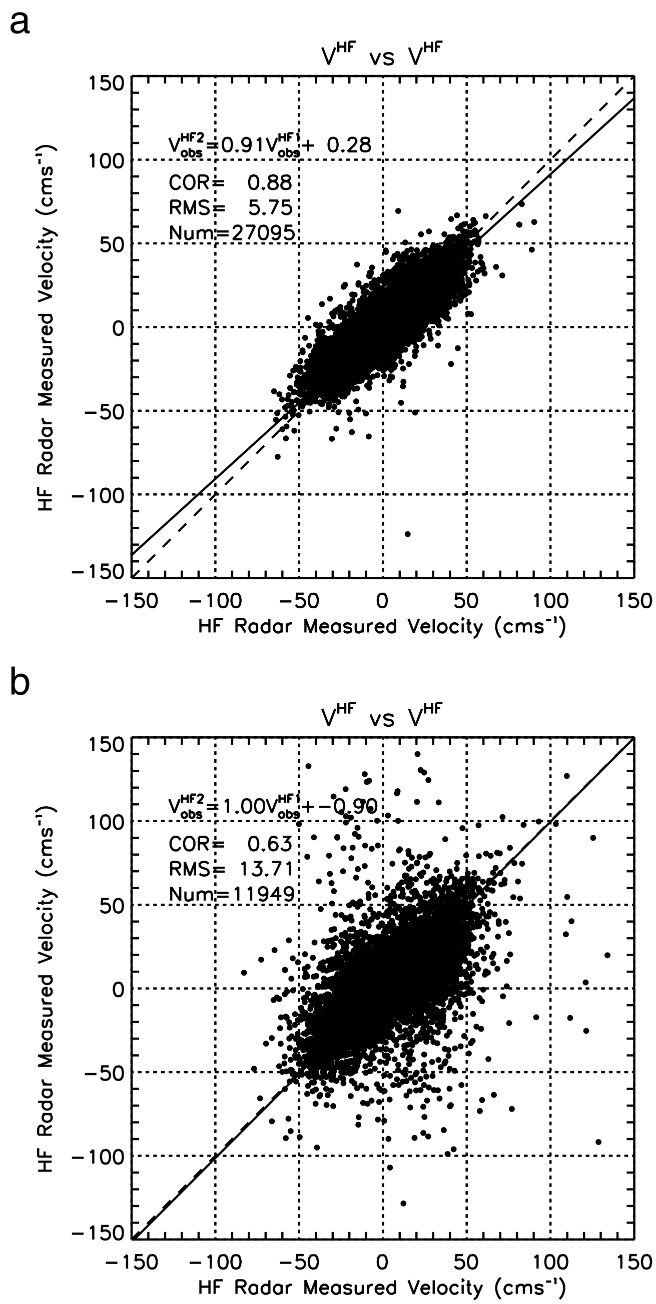

Figure 6. Scatterplots of radial velocities measured by two facing HF radars. (a) C1–C2 comparison. (b) C1–C3 comparison. Solid line is the regression line obtained with PCA.

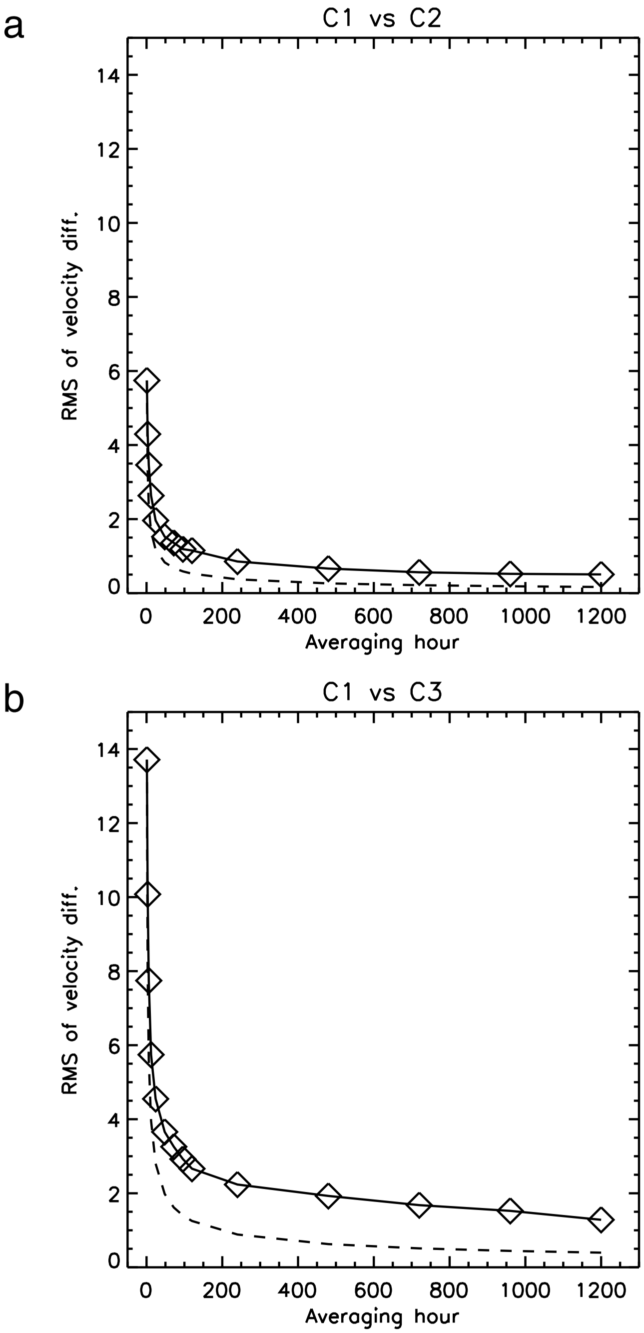

Figure 7. RMS obtained from facing radar comparisons as a function of ensemble number of averaging. (a) C1–C2 comparison. (b) C1–C3 comparison. Dashed line represents inverse of square root of ensemble number.

the radar site increases. This might also be related to the C3 site location, which is far from the coastline, causing the signal-to-noise ratio to be further reduced.

[18] The above results indicate that the variance error of the hourly radial velocity of HF radar (CODAR) is 5.75∼13.7 cm s^{-1} in the Tsushima Strait. The HF radar of NJRC is also expected to have a similar variance error because a comparison with ADCP does not show a significant difference between CODAR and NJRC (Table 3). It should be noted here that the RMS between facing radars (5.75∼13.7 cm s^{-1}) can explain much of the RMS between HF radar and ADCP (6.62∼11.3 cm s^{-1}). This result suggests that HF radar measurement error is the dominant source of velocity difference between HF radar and ADCP. Note also that the SDV obtained from the comparison with ADCP is similar to that of previous studies. This implies that other HF radar systems might contain similar variance error.

5. Discussion

5.1. Variance Error

[19] CODAR estimates not only the radial velocity but also its uncertainty. One method for reducing large variance error is to discard the radial velocity with the larger uncertainty value. If a radial velocity with an uncertainty value larger than 10 cm s^{-1} is discarded, then the RMS obtained from the facing radar comparison reduces from 5.75 to 5.11 cm s^{-1} for the C1–C2 comparison and from 13.7 to 9.31 cm s^{-1} for the C1–C3 comparison, although the number of available data decreases by 8.99% for the C1–C2 comparison and by 34.0% for the C1–C3 comparison. The fact that the RMS of the C1–C3 comparison becomes smaller than the imposed upper limit of uncertainty (10 cm s^{-1}) indicates that quality control based on the uncertainty value works well. A comparison between ADCP and HF radar was also done using only a radial velocity with a uncertainty value smaller than 10 cm s^{-1}, and this showed that the RMS with the Furuno ADCP reduces from 11.3 to 10.3 cm s^{-1} while the RMS with the RD ADCP increases from 6.62 to 7.34 cm s^{-1}. The latter increase is probably related to lower statistical accuracy due to the smaller number of samples.

[20] Another method for reducing variance error is to take the ensemble average since variance errors are expected to be uncorrelated with each other and therefore averaging is expected to reduce them by the square root of the ensemble number. Figure 7 shows the RMSs of averaged radial velocity as a function of the ensemble number. The RMSs of both the C1–C2 and C1–C3 pairs rapidly decrease as the ensemble number increases, although the decrease is slower than the square root of the ensemble number. The RMS reduces to 1.96 cm s^{-1} (C1–C2) and 4.55 cm s^{-1} (C1–C3) if the average is taken over 24 ensembles (daily mean) and it reduces to 0.56 cm s^{-1} (C1–C2) and 1.68 cm s^{-1} (C1–C3) if the average is taken over 720 ensembles (monthly mean).

5.2. Bias Error

[21] Although variance error is reduced by averaging, bias error is not. Figure 8 shows the mean radial velocities along the baseline of the two facing radars as a function of the distance from a radar. Note that the target difference, which is negligible at the middle of baseline, increases toward the ends of the baseline because one radar measures a much larger area than the other as the target grid goes away from the middle of baseline [*Lipa*, 2003]. Velocity differences at the middle of baseline are 0.04 cm s^{-1} for the C1–C2 comparison and 0.65 cm s^{-1} for the C1–C3 comparison. Near the C1 site, the difference between the C1 and C2 velocity amounts to 8.40 cm s^{-1} (Figure 6a). The C1 site is located at the tip of a small island, and thus the C1 radar might measure weak currents near stagnant point while the C2 radar measures broad and strong currents

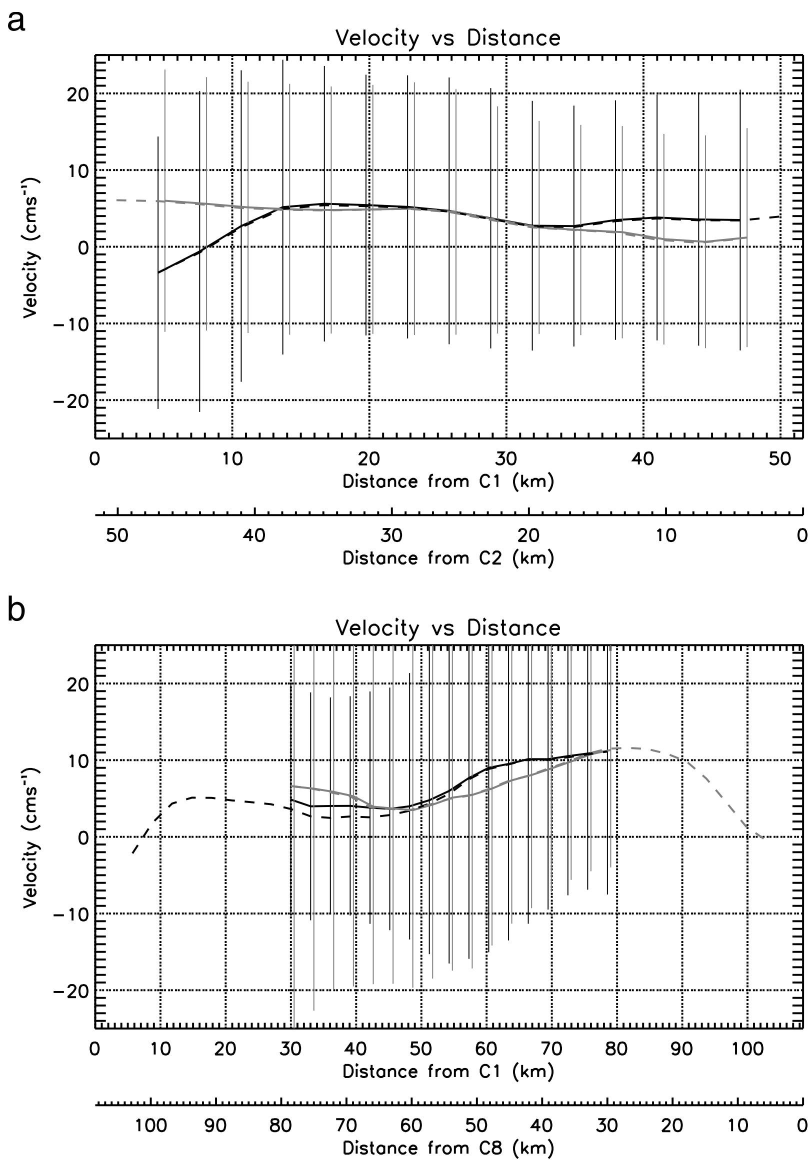

Figure 8. Averaged radial velocities along a baseline between two facing radars. (a) C1 (black) and C2 (gray) (1 February 2002 to 30 April 2005). (b) C1 (black) and C3 (gray) (1 July 2003 to 30 April 2005). Vertical bar denotes standard deviation. Solid line represents average taken over the time when both C1 and C2 or C3 measure radial velocity. Dashed line represents simple average during the period (average taken even if only one radar measures radial velocity).

toward C1. Thus part of this difference near the C1 site might be the target difference. In other regions, the mean velocity difference is generally less than a few centimeters per second.

[22] As described in section 2, antenna pattern distortion causes bearing error and hence significant bias error of radial velocity in CODAR. If radial velocity is estimated with an ideal antenna pattern (i.e., without correcting antenna pattern distortion), the difference between averaged radial velocities increases over almost the entire baseline (Figure 9). The difference at the middle of baseline amounts to 3.23 cm s^{-1} in the C1–C2 comparison and to 2.10 cm s^{-1} in the C1–C3 comparison if an ideal antenna pattern is used. The large velocity difference is due to the bias error of bearing estimation, indicating that radial velocity with an ideal antenna pattern is not actually the velocity along the baseline. Table 4 also shows comparison statistics of the radial velocity estimated with an ideal antenna pattern. It was found that the use of a measured antenna pattern makes the comparison results better in general. Since the correction of antenna pattern distortion should improve bias error, improvements in regression coefficients represent the extent to which the distortion is corrected. For this reason, we consider here that the use of a measured antenna pattern is better than the use of an ideal antenna pattern in the C1–C3 comparison, even though RMS is larger for the former than for the latter. In the C1–C2 comparison, the use of a measured antenna pattern makes the slope of the regression line worse, while the intercept of the line improves greatly. This suggests that antenna pattern distortion along

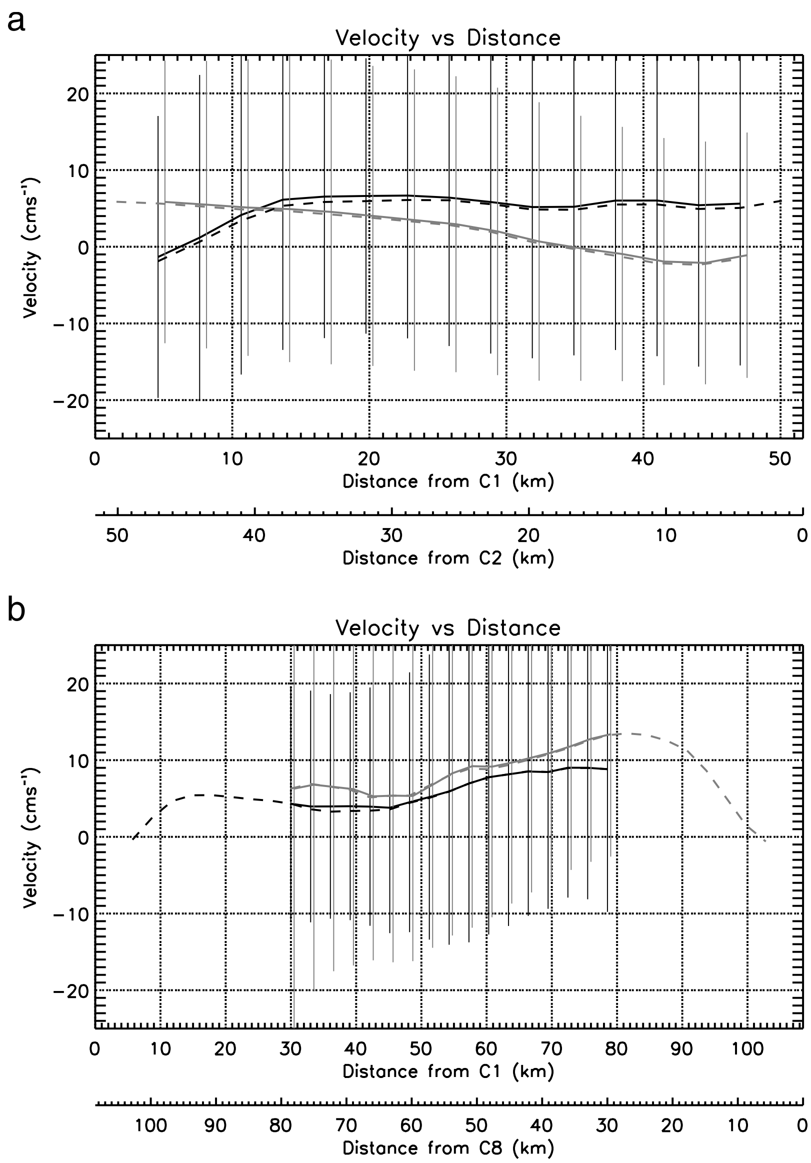

Figure 9. Same as Figure 8 but for radial velocities estimated with an ideal antenna pattern.

Table 5. C1–C2 Comparison Between $v_1(r_{12}/2,\ \theta_{12} + \Delta\theta_1)$ and $v_2(r_{12}/2,\ \theta_{21} + \Delta\theta_2)$[a]

		$\Delta\theta_1$		
$\Delta\theta_2$	Statistics	−5°	0°	+5°
−5°	A	0.94	0.86	0.78
−5°	B	0.95	0.99	0.88
−5°	RMS	5.88	5.96	6.40
0°	A	1.00	0.91	0.83
0°	B	0.24	0.28	0.14
0°	RMS	5.67	5.75	6.21
+5°	A	1.05	0.96	0.88
+5°	B	−0.49	−0.46	−0.63
+5°	RMS	5.72	5.73	6.18

[a]Here, $v_i(r, \theta)$ is radial velocity of radar i at range r and bearing angle θ with r_{ij} and θ_{ij} is distance between Ci and Cj and bearing angle from Ci to Cj, respectively. A, B, RMS represent slope and intercept of regression line and RMS, respectively.

the C1–C2 baseline is not perfectly corrected in spite of the use of a measured antenna pattern [*Paduan et al.*, 2006].

[23] To examine this possibility, the facing radar comparison with the measured antenna pattern was extended to include a comparison of radial velocities at several angles on the same range (half of the baseline distance) arc [*Paduan et al.*, 2006]. Mathematically, $v_1(r_{1i}/2,\ \theta_{1i} + \Delta\theta_1)$ and $v_i(r_{i1}/2, \theta_{i1} + \Delta\theta_i)$ are compared ($i = 2, 3$), where $v_j\,(r, \theta)$ is

Table 6. Same as Table 5 Except for C1–C3 Comparison

		$\Delta\theta_1$		
$\Delta\theta_3$	Statistics	−5°	0°	+5°
−5°	A	1.14	0.91	0.88
−5°	B	−4.00	−2.25	−0.48
−5°	RMS	14.3	15.0	15.4
0°	A	1.22	1.00	0.97
0°	B	−2.66	−0.90	1.11
0°	RMS	13.2	13.7	14.2
+5°	A	1.21	1.00	0.97
+5°	B	−0.81	0.72	2.65
+5°	RMS	12.8	13.3	13.9

Table 7. Amplitude, Phase, and Direction of Major Diurnal Tidal Ellipses Obtained in This Study and by *Takikawa et al.* [2003]

	HF radar			ADCP			Difference		
	Amp, cm s^{-1}	Phase, deg	Dir, deg	Amp, cm s^{-1}	Phase, deg	Dir, deg	Amp, %	Phase, %	Dir, %
K_1	12.8	283	41	13.0	279	36	1.56	2.2	2.8
O_1	10.3	253	39	11.1	253	35	0.78	0.0	2.2

radial velocity measured by Cj radar (j = 1, 2, 3) at range r and bearing angle θ with $r_{1i}(= r_{i1})$ and $\theta_{1i}(= \theta_{i1} + 180°)$ being the distance between C1 and Ci and the bearing from C1 to Ci, respectively. Note that the facing radar comparison in section 5.1 corresponds to $\Delta\theta_i = 0$. Tables 5 and 6 shows the regression coefficients and RMS obtained from this comparison with $\Delta\theta_i = -5°, 0°, 5°$. The best regression coefficients are obtained between $\Delta\theta_1 = -5°$ and $\Delta\theta_2 = 0°$ (negative bearing represents clockwise rotation) in the C1–C2 comparison and between $\Delta\theta_1 = 0°$ and $\Delta\theta_3 = 5°$ in the C1–C3 comparison. These results clearly show that the use of a measured antenna pattern does not perfectly correct antenna pattern distortion [*Paduan et al.*, 2006]. These results also show that bearing bias is a function of bearing angle, since the $\Delta\theta_1$ differs between the C1–C2 and C1–C3 comparisons.

[24] It should be remembered here that bias error is partly cancelled in the facing radar comparison. Thus the whole bias error should be examined by intercomparison between HF radar and other instruments (such as ADCP), with particular attention paid to the large variance error of HF radar measurement and the target difference. To this aim, we compared tidal ellipses estimated from the long-term measurement of HF radar and ADCP measurements by *Takikawa et al.* [2003]. The variance error was expected to be negligible because the amount of data is large. The target difference was also expected to be small because tidal currents are originally barotropic, and wind stress (which induces vertical shear near the sea surface) is expected to be weak at tidal frequencies.

[25] The tidal ellipses of *Takikawa et al.* [2003] are estimated from 5 years of ADCP measurement along a ferryboat track across the Tsushima Strait, and their averages along the track were used for comparison in this study. The tidal ellipses estimated from HF radar along the ferryboat track were obtained by harmonic analysis of hourly radial velocities from July 2003 to June 2004. Unfortunately, HF radar measurement covers only the eastern half of the ferryboat track. Therefore the tidal ellipses of major diurnal tides (K_1 and O_1), which differ little between the eastern and western channels, were compared (Table 7).

[26] Very good agreement between the HF radar measurement and ADCP measurement was found. Differences in amplitude, phase, and direction were less than 0.8 cm s^{-1}, 4°, and 5°, respectively. These differences are less than a few percent. Although the bias error of the HF radar measurement remains, it is considered to be reasonably small at least for the major diurnal tides along the ferryboat track.

6. Summary

[27] We investigated the accuracy of HF radar measurement by comparing velocities measured by HF radar and ADCP, and also by comparing velocities measured by two facing HF radars. A comparison with ADCP, which provides an upper bound of HF radar measurement error, showed that the root-mean-square (RMS) of velocity difference obtained from PCA was 6.62∼11.3 cm s^{-1}. These values are similar to those of previous studies. A comparison between the two facing HF radars, which gives a lower bound of HF radar measurement error, showed that the RMS of hourly radial velocity was 5.75∼13.7 cm s^{-1}. This is large enough to explain the RMS between HF radar and ADCP. Thus it was concluded that the dominant source of velocity difference between HF radar and ADCP in this study was the HF radar variance error.

[28] It was confirmed that ensemble averaging reduces variance error as the ensemble number increases. In the present study, daily averaging reduced more than 65% of the variance error of hourly radial velocity. The uncertainty of radial velocity estimation (an output of the CODAR system) is also useful for reducing the variance error of CODAR. The use of a measured antenna pattern corrects antenna pattern distortion and reduces the bias error of CODAR, but the correction was not perfect in this study. The total bias error of HF radar measurement was examined by comparing the major diurnal tidal ellipses estimated from 1 year of HF radar data and 5 years of ADCP data obtained along a ferryboat track across the Tsushima Strait. Very good agreement between them suggests that the bias error of HF radar measurement is reasonably small, at least along the ferryboat track.

[29] The major error of the hourly radial velocity of HF radar is thus the variance error rather than the bias error. The development of schemes that reduce this variance error is therefore necessary and will be the focus of our future work.

[30] **Acknowledgments.** We wish to express our thanks to the captain, officers, and all crew members of the T/V *Kakuyo-Maru* of Nagasaki University and R/B Danryu. We would also like to express our thanks to the 7th Regional Coast Guard Headquarters and the Fukuoka Fisheries and Marine Technology Research Center for their support of this study. Satoshi Fujii of Ryukyu University gave us instructive comments about HF radar operating theory. Part of this study is supported by Grant-in-Aid for Scientific Research (B) of the Ministry of Education, Culture, Sports, Science and Technology.

References

Barrick, D. E., and B. J. Lipa (1997), Evolution of bearing determination in HF current mapping radars, *Oceanography*, *10*, 72–75.

Barrick, D. E., M. W. Evans, and B. L. Weber (1997), Ocean surface currents mapped by radar, *Science*, *198*(C8), 138–144.

Chapman, R. D., L. K. Shay, H. C. Graber, J. B. Edson, A. Karachintsev, C. L. Trump, and D. B. Ross (1997), On the accuracy of HF radar surface current measurements: Intercomparisons with ship-based sensors, *J. Geophys. Res.*, *102*(C8), 18,737–18,748.

Graber, H. C., B. K. Haus, R. D. Chapman, and L. K. Shay (1997), HF radar comparisons with moored estimates of current speed and direction: Expected differences and implications, *J. Geophys. Res.*, *102*(C8), 18,749–18,766.

Holbrook, J. R., and A. S. Frisch (1981), A comparison of near-surface CODAR and VACM measurements in the strait of Juan De Fuca, August 1978, *J. Geophys. Res.*, *86*(C11), 10,908–10,912.

Lipa, B. J. (2003), Uncertainties in Seasonde current velocities, paper presented at the IEEE/OES Seventh Working Conference on Current Measurement Technology, Inst. of Electr. and Electron. Eng., San Diego, Calif.

Lipa, B. J., and D. E. Barrick (1983), Least-squares methods for the extraction of surface currents from CODAR cross-loop data: Application at ARSLOE, *IEEE J. Oceanic Eng.*, *OE8*, 226–253.

Matthews, J. P., J. H. Simpson, and J. Brown (1988), Remote sensing of shelf sea currents using a high-frequency ocean surface current radar system, *J. Geophys. Res.*, *93*(C3), 2303–2310.

Nadai, A., H. Kuroiwa, M. Mizutori, and S. Sakai (1997), Measurement of ocean surface currents by CRL HF ocean surface radar of the FMCW type. part 1. Radial current velocity, *J. Oceanogr. Soc. Jpn.*, *53*, 325–342.

Odamaki, M. (1989), Tides and tidal currents in the Tusima strait, *J. Oceanogr. Soc. Jpn.*, *45*, 65–82.

Paduan, J. D., and H. C. Graber (1997), Introduction to high frequency radar: Reality and myth, *Oceanography*, *10*(2), 36–39.

Paduan, J. D., K. C. Kim, M. S. Cook, and F. P. Chavez (2006), Calibration and validation of direction-finding high frequency radar ocean surface current observations, *IEEE J. Oceanic Eng.*, in press.

Takikawa, T., J. H. Yoon, and K. D. Cho (2003), Tidal currents in the Tsushima Straits estimated from ADCP data by ferryboat, *J. Oceanogr. Soc. Jpn.*, *59*, 37–47.

M. Ishibashi, K. Marubayashi, A. Masuda, and Y. Yoshikawa, Research Institute for Applied Mechanics, Kyushu University, 6-1 Kasuga Park, Kasuga, Fukuoka, 816-8580, Japan. (yosikawa@riam.kyushu-u.ac.jp)

A. Okuno, National Research Institute of Fisheries Sciences, Fisheries Research Agency, 2-12-4 Fukuura, Kanazawa, Yokohama, Kanagawa, 236-8648, Japan.